PALEOECOLOGY

Extinction at the end-Cretaceous and the origin of modern Neotropical rainforests

Mónica R. Carvalho[1,2]*, Carlos Jaramillo[1,3,4]*†, Felipe de la Parra[5], Dayenari Caballero-Rodríguez[1], Fabiany Herrera[1,6], Scott Wing[7], Benjamin L. Turner[1,8], Carlos D'Apolito[1,9], Millerlandy Romero-Báez[1,10], Paula Narváez[1,11], Camila Martínez[1], Mauricio Gutierrez[1,12], Conrad Labandeira[7,13,14], German Bayona[15], Milton Rueda[16], Manuel Paez-Reyes[1,17], Dairon Cárdenas[18], Álvaro Duque[19], James L. Crowley[20], Carlos Santos[21], Daniele Silvestro[22,23]

The end-Cretaceous event was catastrophic for terrestrial communities worldwide, yet its long-lasting effect on tropical forests remains largely unknown. We quantified plant extinction and ecological change in tropical forests resulting from the end-Cretaceous event using fossil pollen (>50,000 occurrences) and leaves (>6000 specimens) from localities in Colombia. Late Cretaceous (Maastrichtian) rainforests were characterized by an open canopy and diverse plant–insect interactions. Plant diversity declined by 45% at the Cretaceous–Paleogene boundary and did not recover for ~6 million years. Paleocene forests resembled modern Neotropical rainforests, with a closed canopy and multistratal structure dominated by angiosperms. The end-Cretaceous event triggered a long interval of low plant diversity in the Neotropics and the evolutionary assembly of today's most diverse terrestrial ecosystem.

Paleontological evidence indicates that the bolide impact at Chicxulub, 66.02 million years ago (Ma) (*1*), had immediate catastrophic effects on plant communities and reshaped terrestrial ecosystems worldwide (*2*–*4*). Despite the extent of this ecological disruption, the long-term extinction and recovery patterns were geographically heterogeneous (*5*). As much as 90% of pre-extinction palynomorphs reappeared during the Danian (66 to 61.6 Ma) in Patagonia and New Zealand (*6*, *7*), and species-rich Danian megafloral assemblages with diverse types of insect damage indicate rapid recovery of diversity in Patagonia (*8*, *9*). By contrast, palynofloral extinction was up to 30% in the Northern Great Plains of North America (*10*), and floral and insect-damage diversity may not have reached pre-extinction levels until the latest Paleocene or early Eocene [(*11*, *12*); but see (*3*)].

Phylogenies of several plant lineages suggest that the Cretaceous–Paleogene (K/Pg) event marking the end of the Cretaceous played a role in shaping modern tropical lowland rainforests (*13*–*15*), but the fate of tropical forests following the K/Pg boundary is not well understood. Assessing plant extinction and recovery requires a thoroughly sampled fossil record, yet aside from an impact-related fern-spore spike in deep-water strata from Gorgonilla, Colombia (*16*), the plant fossil record across the K/Pg boundary in the lowland Neotropics is sparse (*17*). Here, we quantify changes in the diversity, structure and composition of forests across the K/Pg boundary in tropical South America using a palynological dataset spanning the Maastrichtian–Paleocene interval, including 39 stratigraphic sections from outcrops and wells, 637 samples, 1048 taxa, and 53,029 occurrences (Fig. 1 and table S1) (*18*). As fossil pollen assemblages typically integrate information at large spatial scale (i.e., tens of square kilometers), we also examined the composition and diversity of autochthonous assemblages of leaf fossils, which instead reflect local forest communities. These included 2053 fossils from the Maastrichtian Guaduas Formation and 4898 fossils from the middle-late Paleocene Bogotá and Cerrejón formations (*19*). Situated near the paleo-equator, this then-coastal region of northern South America was wet and megathermal throughout the globally warm Maastrichtian and Paleocene. As a result, the effect of the end-Cretaceous event on the fossil record is not confounded by major changes in climate.

Extinction and turnover of tropical vegetation

We estimated diversity using the corrected sampled-in-bin diversity (*20*), the shareholder quorum subsampling (SQS) (*21*), origination and

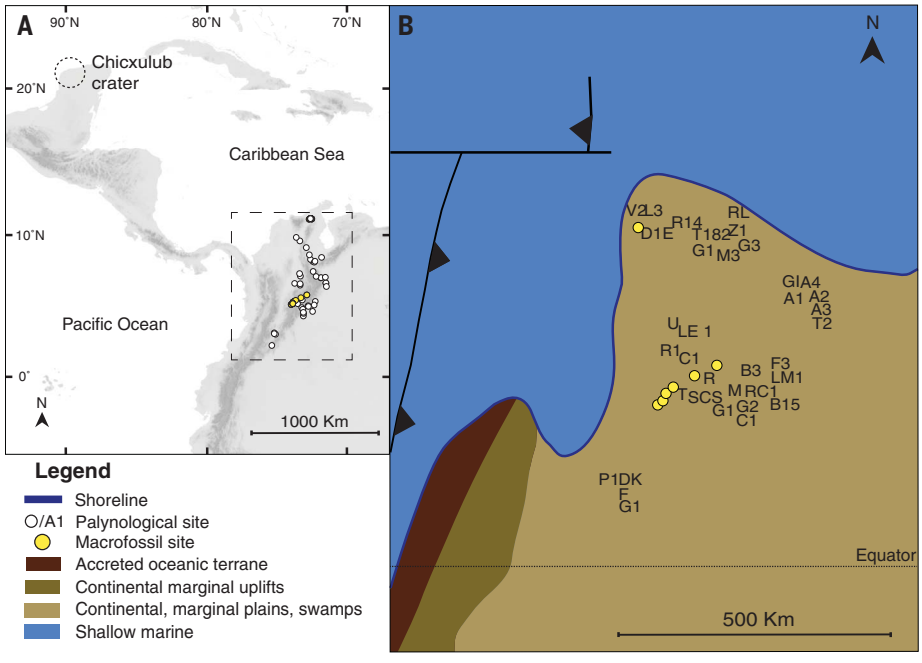

Fig. 1. Location of stratigraphic sections and macrofossil localities in northern South America. (**A**) Map showing modern-day distance to Chicxulub crater. (**B**) Paleogeographic reconstruction of northern South America [area delimited by dotted rectangle in (A)] during the late Maastrichtian, based on (*64*).

[1]Smithsonian Tropical Research Institute, Panama. [2]Grupo de Investigación Paleontología Neotropical Tradicional y Molecular (PaleoNeo), Facultad de Ciencias Naturales y Matemáticas, Universidad del Rosario, Bogotá, Colombia. [3]ISEM, U. Montpellier, CNRS, EPHE, IRD, Montpellier, France. [4]Department of Geology, Faculty of Sciences, University of Salamanca, Salamanca, Spain. [5]Instituto Colombiano del Petróleo, Bucaramanga, Colombia. [6]Negaunee Institute for Plant Conservation, Chicago Botanic Garden, Chicago, IL, USA. [7]Department of Paleobiology, National Museum of Natural History, Washington, DC, USA. [8]Soil and Water Science Department, University of Florida, Gainesville, FL, USA. [9]Faculdade de Geociências, Universidade Federal de Mato Grosso, Cuiabá, Brazil. [10]ExxonMobil Corporation, Spring, TX, USA. [11]Instituto Argentino de Nivología, Glaciología y Ciencias Ambientales, CCT-CONICET, Mendoza, Argentina. [12]Departamento de Geología, Universidad de Chile, Santiago, Chile. [13]Department of Entomology, University of Maryland, College Park, MD, USA. [14]College of Life Sciences, Capital Normal University, Beijing, China. [15]Corporación Geológica Ares, Bogotá, Colombia. [16]Paleoflora Ltda, Zapatoca, Colombia. [17]Department of Earth and Atmospheric Sciences, University of Houston, Houston, TX, USA. [18]Instituto Amazónico de Investigaciones Científicas SINCHI, Leticia, Colombia. [19]Departamento de Ciencias Forestales, Universidad Nacional de Colombia, Medellín, Colombia. [20]Department of Geosciences, Boise State University, Boise, ID, USA. [21]BP Exploration Operating Company Limited, Chertsey Road, Sunbury-on-Thames, Middlesex, UK. [22]Department of Biology, University of Fribourg, Fribourg, Switzerland. [23]Department of Biological and Environmental Sciences, University of Gothenburg and Gothenburg Global Biodiversity Centre, Gothenburg, Sweden.
*These authors contributed equally to this work.
†Corresponding author. Email: jaramilloc@si.edu

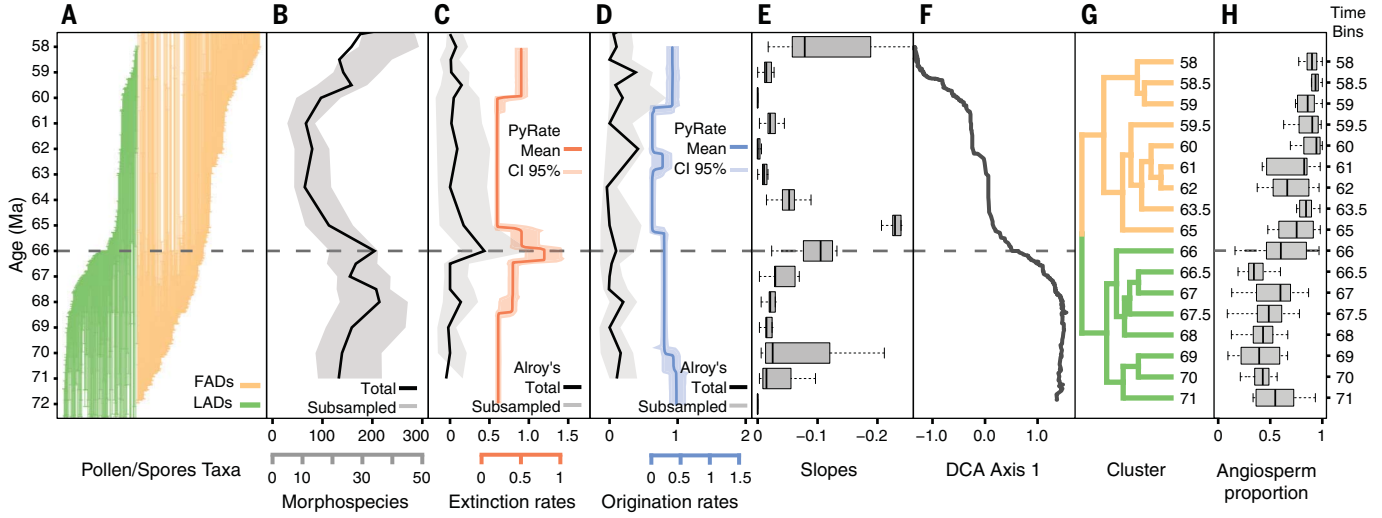

Fig. 2. Changes in diversity and composition of Maastrichtian-Paleocene palynofloras in northern South America. (**A**) Stratigraphic ranges of taxa across the Maastrichtian-Paleocene interval. Shown in green are the taxa that became extinct and in orange, the taxa that originated during this time period. (**B**) Corrected sampled-in-bin diversity. (**C**) PyRate (*23*) extinction rate mean and 95% credible interval (orange shadow) and Alroy's second-for-third (*22*) extinction rate. (**D**) PyRate origination rate mean and 95% credible interval (blue shadow), and Alroy's second-for-third origination rates with 0.95 confidence interval (SQS = 0.95; gray shadow). (**E**) Boxplot of slopes from the survivorship analysis performed on 1-million-year bin cohorts. (**F**) Change in floral composition shown by scores of samples on DCA axis 1 plotted against time. (**G**) Sørensen Cluster showing two distinct clusters, Maastrichtian (green) and Paleocene (orange); see fig. S1 for individual samples cluster. (**H**) Boxplot of the proportion per bin of angiosperm grains versus total flora; see fig. S2 for proportion of individual samples.

extinction rates using the second-for-third method (*22*), and PyRate (*23*) [see materials and methods (*18*)]. Palynofloral diversity was higher in the Maastrichtian (72 to 66 Ma) in tropical South America than in the early and middle Paleocene (66 to 60 Ma) (Fig. 2B; mean of Maastrichtian bins 172.3 versus Paleocene bins 84.1, *t* test, df = 10.9, $P < 0.001$; table S3), regardless of differences in sampling size (Fig. 2B, SQS estimates 27 versus 12.7, *t* test, df = 3872.7, $P < 0.001$) or depositional environments (table S4). This marked decrease in diversity coincides with a peak in extinction rates at 66 Ma (66 to 66.5 age bin; log Bayes factors >6 with a 95% credible interval between 66.4 and 65.7) that diminishes palynomorph diversity by 45% and significantly exceeds Maastrichtian or Paleocene background extinction (Fig. 2C, extinction rate of 0.44 versus a mean of 0.04 for all other bins, SQS estimates 0.53 versus 0.03, *t* test, df = 309.08, $P < 0.001$; PyRate extinction rate 0.75; credible interval (CI): 0.45 to 1 versus a median rate of 0.07; CI: 0.04 to 0.09 in the Maastrichtian and 0.05; CI 0.03 to 0.07 in the early Paleocene). As a result, most Maastrichtian cohorts (groups of palynomorphs that coexist at a given time) decline in the first bin of the Paleocene (65 Ma bin), well above the mean cohort reduction observed throughout the Paleocene (Fig. 2E, mean slope of all cohorts at 65 bin 0.24 versus mean slope of all other cohorts, 0.05, *t* test, df = 13, $P < 0.001$).

Following the K/Pg boundary, palynomorph diversity did not recover to pre-extinction levels until after 60 Ma (Fig. 2B) and further increased beyond pre-extinction levels throughout the Paleocene–Eocene Thermal Maximum and early Eocene (*24*, *25*). The second-for-third estimates identify a peak in origination during the 59- to 59.5-Ma interval (Fig. 2D; mean origination rate 0.38, mean at all other intervals 0.09; SQS estimates 0.95, 0.28 versus 0.08, *t* test, df = 332.54, $P < 0.001$), whereas PyRate found support (log Bayes factors >6) for a drop in origination in the earliest Paleocene (from 0.23; CI: 0.2 to 0.27 to 0.04; CI: 0.01 to 0.08) and a strong increase between 60.7 and 60.2 Ma (rate 0.37; CI: 0.28 to 0.47). A reanalysis of the data allowing the PyRate algorithm to search for rate shifts at a higher temporal resolution resulted in similar patterns of origination and extinction overall (fig. S3). However, the analysis detected an additional brief but strong peak in origination rates between 59.6 and 59.2 Ma, when the origination rates increased from 0.26 (CI: 0.18 to 0.38) to 1.30 (CI: 0.90 to 1.72).

We used detrended correspondence analysis (DCA) and cluster analysis to evaluate changes in palynofloral composition across the K/Pg boundary. Rapid change through time in the first axis scores of samples (Fig. 2F, first axis explains 57% of variation) and a distinct clustering of Maastrichtian and Paleocene plant communities (Fig. 2G and fig. S1) reflect a major and permanent change in floristic composition. Although the Maastrichtian contained roughly equal proportions of angiosperm (47.9%) and spore grains (49.5%), angiosperm grains dominated in the Paleocene (mean abundance 84% versus 16% of non-angiosperms, Wilcoxon test, W-statistic = 14,552, $P < 0.001$; fig. S2). Gymnosperms (mostly Araucariaceae) are 2.5% of Maastrichtian grains but only 0.4% of Paleocene grains (Mann-Whitney test, U-statistic = 17,509, $P < 0.01$). Gymnosperms also occur in 75% of Maastrichtian samples but only in 24% of Paleocene samples having >100 grains. Sediments from the Maastrichtian Umir Formation (central Colombia) are rich in gymnosperm lipid biomarkers (*26*), supporting the abundance of gymnosperms prior to the K/Pg extinction. Living species of Araucariaceae occur as large trees and are often underrepresented in the palynological soil record and do not disperse long distances (*27*), such that their low abundance in Maastrichtian deposits is likely to be an underestimation of their true abundance.

Leaf physiognomy and forest types

We recognize 41 angiosperm and 4 fern morphotypes in the Maastrichtian Guaduas macroflora. In the Paleocene, we found 46 angiosperms and 2 ferns in the Bogotá flora and 58 angiosperms, 5 ferns, and 1 conifer leaf morphotype in the Cerrejón flora. The foliar physiognomy of nonmonocot angiosperm leaves (ANA-grade angiosperms: Amborellales, Nymphales, and Austrobaileyales; magnoliids; and eudicots) in both the Maastrichtian and Paleocene assemblages resembles that of modern tropical rainforests, characterized by leaves of large size, untoothed margins, and elongated drip tips (Fig. 3). Of the 36 species of non-

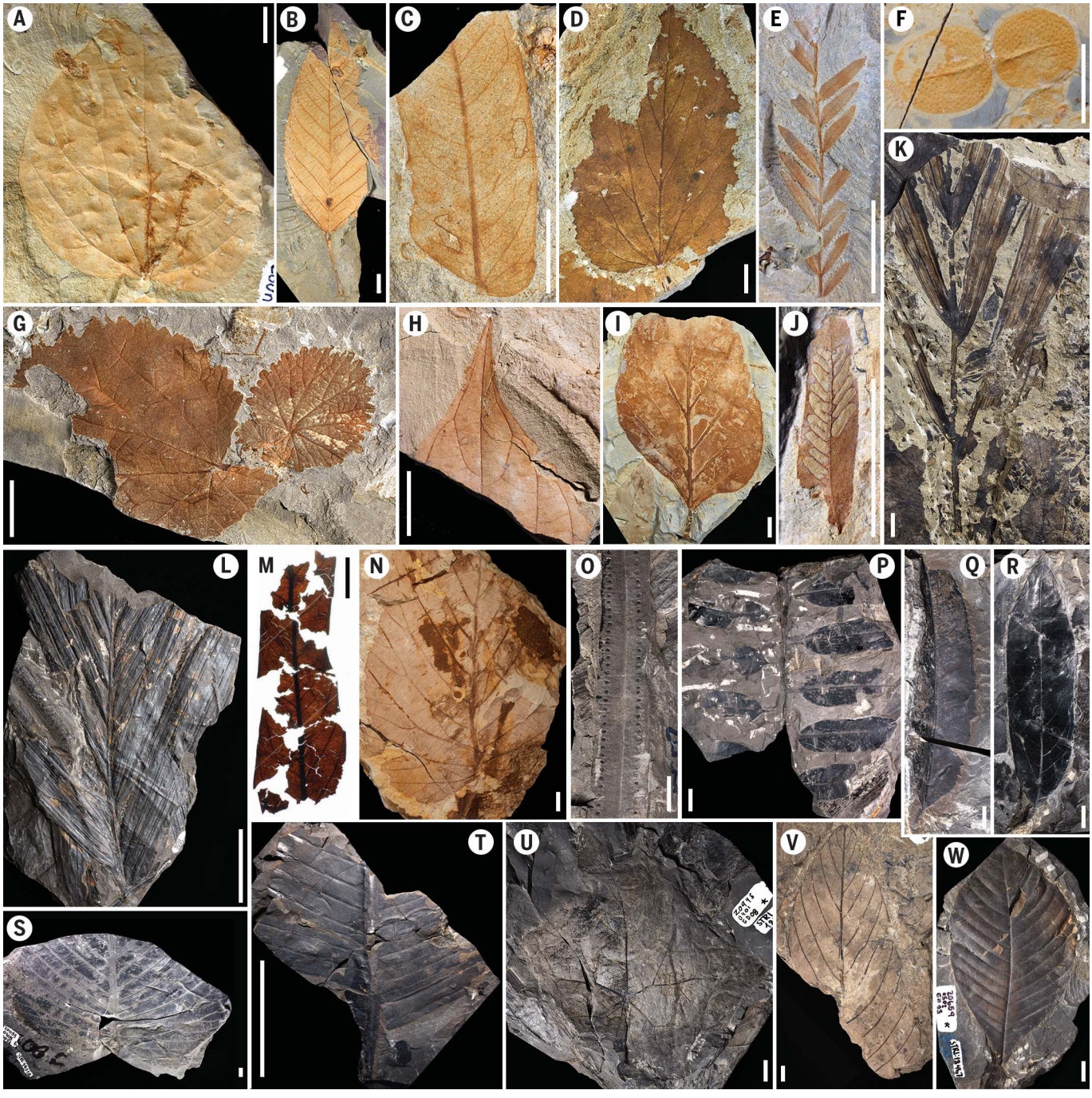

Fig. 3. Representative leaf taxa. (A to K) Taxa from Paleocene Bogotá and (L to W) Maastrichtian Guaduas floras. (**A**) Menispermaceae (BF6). (**B**) Salicaceae (BF5) with midrib gall. (**C**) Fabaceae leaflet (BF38) with surface feeding damage. (**D**) Euphorbiaceae (BF37) with hole and margin feeding. (**E**) Fabaceae, Caesalpinioideae (BF21). (**F**) Water fern, *Salvinia bogotensis*, Salviniaceae (BF22). (**G**) *Malvaciphyllum* sp. Malvaceae (BF4). (**H**) Example of drip tip in Salicaceae (BF23). (**I**) aff. Eleaocarpaceae (BF13). (**J**) Fabaceae leaflet (BF21, 5 mm) with hole feeding damage. (**K**) Arecaceae (BF27). (**L**) Arecaceae (GD47, 10 cm). (**M**) aff. Lauraceae (GD54). (**N**) aff. Hamamelidaceae (GD56). (**O** and **P**) Fertile and sterile fragments of Polypodiaceae (GD22). (**Q**) aff. Salicaceae (GD6). (**R**) Lauraceae (GD7) with drip tip. (**S**) aff. Urticaceae (GD52). (**T**) Zingiberales (GD46, 5 cm). (**U**) aff. Cucurbitaceae (GD8). (**V**) *Bernhamniphyllum* sp. Rhamnaceae (GD1). (**W**) aff. Dilleniaceae (GD3). Scale bars: 1 cm except where noted in parentheses after taxon.

monocots in the Guaduas flora, 89% have leaves larger than 45 cm^2 (mesophylls), 81% have untoothed margins, and 11 of the 25 species with preserved apices have drip tips (44%). In the Paleocene assemblages, 63 and 76% of nonmonocot species have untoothed margins (Bogotá and Cerrejón, respectively), and 30 to 35% have elongated drip tips. Estimates of mean annual rainfall based on Leaf Area Analysis (*18*, *28*, *29*) indicate annual precipitation of 234 to 293 cm $year^{-1}$ for the Guaduas flora, 182 to 184 cm $year^{-1}$ for the Bogotá flora, and 240 to 308 cm $year^{-1}$ for the Cerrejón flora (Table 1 and table S8).

Leaf mass per area (LMA) values, estimated on the basis of the scaling relationship between leaf mass and petiole diameter observed in living plants (*30*), were consistent with modern

Table 1. Leaf physiognomy and precipitation of the Maastrichtian-Paleocene floras. Numbers in parentheses indicate numbers of quarries (Total specimens), number of census localities (Census), and number of morphotypes with preserved apices (drip tips). MAP, mean annual precipitation.

Formation	Age	Total specimens	Census numbers	Leaf taxa	Nonmonocot taxa	Non-monocots with entire margins	Nonmonocots with drip tips	Leaves mesophylls or larger	MAP (cm year^{-1})
Guaduas	Maastrichtian	2053 (12)	1650 (2)	45	36	29 (81%)	11 (25)	32 (89%)	234–293
Bogotá	Paleocene	2416 (19)	1370 (1)	48	40	25 (63%)	6 (20)	25 (63%)	182–184
Cerrejón*	Paleocene	2482 (18)	1190 (2)	65	46	35 (76%)	12 (34)	44 (68%)	240–304

*Data reported by (*19*).

evergreen rainforest environments across all three floras (Guaduas: 36 to 206 g m^{-2}; Bogotá: 52 to 206 g m^{-2}; Cerrejón: 44 to 126 g m^{-2}), yet LMAs of the Guaduas and Bogotá floras are lower than those of Cerrejón (*t* test, $P < 0.001$, tables S9 and S10) (*18*). Evergreen trees tend to have higher LMAs when living under drier climates (*31*), which is consistent with the relatively lower precipitation of the Bogotá flora compared with Cerrejón. The Guaduas and Cerrejón floras had similar precipitation (>200 cm year^{-1}), so it is possible that the higher Guaduas LMA may reflect a higher irradiance related to canopy structure (see below) or poorer soils (*31*).

A notable feature of the Paleocene Cerrejón flora is its resemblance to modern Neotropical rainforests in terms of family-level composition of angiosperms (*19*). To examine this, we compared the natural affinities of leaf taxa in the Guaduas with those at Bogotá, Cerrejón, and modern Neotropical rainforests. Some Maastrichtian angiosperms have confirmed or tentative affinities to families that are widely distributed in (but not necessarily restricted to) the lowland tropics, including Lauraceae (two or three morphotypes), Araceae (two morphotypes), Theaceae (one or two morphotypes), Arecaceae, Rhamnaceae (*32*), Piperaceae (*33*), Salicaceae, Canellaceae, Dilleniaceae, Urticaceae, and Monimiaceae (one morphotype each), among others (Fig. 4A, table S6, and data S4). The flowering plants of the Paleocene Bogotá flora closely resemble those of the Cerrejón flora (*19*) and include the dominant tree families in modern Neotropical rainforests. The Bogotá flora has two leaflet types of Fabaceae, one of these representing the earliest record of Caesalpinioideae (with abundant legume pods) (*34*), Euphorbiaceae, Lauraceae, Salicaceae, Violaceae (two morphotypes each), Malvaceae, Melastomataceae (*35*), Rhamnaceae, Arecaceae, Eleaocarpaceae, and Araceae (one morphotype each; table S7 and data S5). Fossil seeds of Annonaceae, Icacinaceae, Menispermaceae, and Passifloraceae are also present in the Bogotá flora. Because nearly autochthonous leaf assemblages reflect tree biomass as a combination of stem abundance and stem diameter (*36*), we compared the family-level composition of five unbiased census sites (two from Guaduas, one from Bogotá, and two from Cerrejón) with permanent plots in two living Neotropical rainforests: Barro Colorado Island (BCI), Panama (*37*), and Amacayacu, Colombia (*38*). In living tropical rainforests, samples of leaf litter that are analogous to single fossil quarry sites can represent most of the standing vegetation (90% biomass) in a 12.5-m radius (*36*). The Paleocene census sites are more similar in family composition to the living forest at BCI (Fig. 4B; Wilcoxon test, W = 46882, $P < 0.001$) and Amacayacu

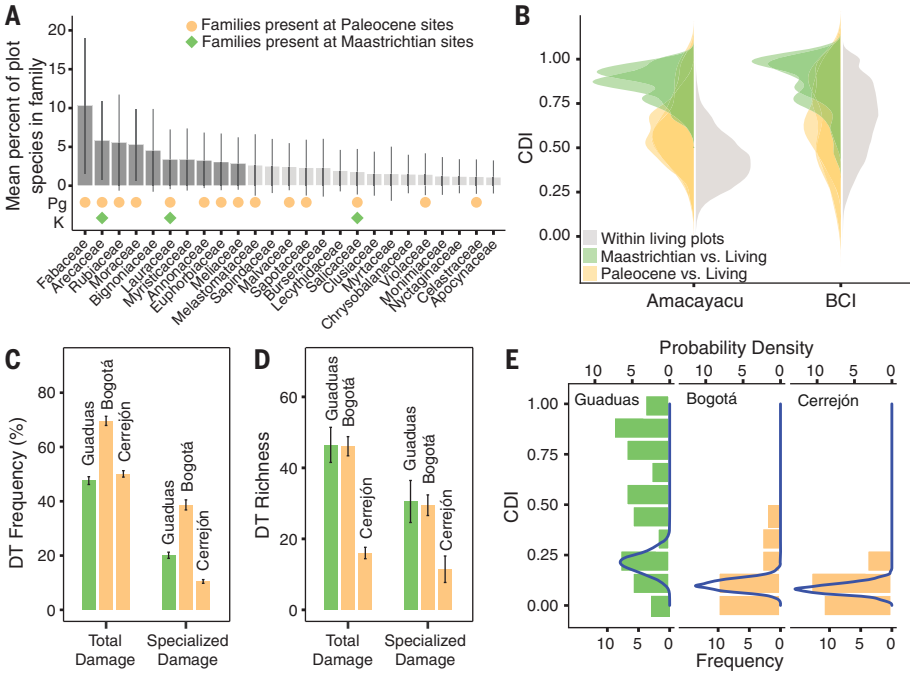

Fig. 4. Forest composition and insect-feeding damage of fossil floras. (**A**) Percentage of tree species in 72 extant Neotropical forest plots that belong to the 25 plant families that together account for 75% of diversity. Half of the stems belong to the 10 families shown as dark bars. Orange circles indicate families present in the Bogotá or Cerrejón floras (Paleocene), and green diamonds indicate families present in the Maastrichtian Guaduas flora. (**B**) Density plot of dissimilarity in family composition between fossil assemblages and samples of living Neotropical forests (see materials and methods for details). Chao-Sørensen dissimilarity (CDI) was calculated between randomly selected subregions of the 50-ha plot at Barro Colorado Island (Panama) and the 25-ha plot at Amacayacu (Colombia). Gray areas depict the distribution of dissimilarities of the randomly selected subregions within each site. (**C**) Average frequency of damaged leaves in 400 randomly selected leaves from each fossil flora. (**D**) Richness of total and specialized insect-mediated damage types, rarefied to 95 and 90% sample coverage, respectively. Gray lines indicate 95% confidence intervals. (**E**) Histogram of leaf damage beta-diversity across host plant species with more than 20 leaves at the Guaduas, Bogotá, and Cerrejón floras. Pairwise beta-diversity was quantified using CDI and is depicted in solid bars. The blue curve indicates the probability density for the null expectation that the observed DTs are randomly distributed across host plant species.

(Wilcoxon test, W = 7806, $P < 0.001$) than they are to the Maastrichtian census sites (fig. S5).

Canopy structure is reflected in the distribution of leaf vein length per area (VLA) and stable carbon isotope ratios ($\delta^{13}C$) within individual taxa (*39*, *40*). Most nonmonocots from Guaduas have relatively high VLA values (*39*, *41*), yet the unimodal distribution of VLA within single taxa in the Guaduas flora (*39*) and the low range of $\delta^{13}C$ measured in leaf cuticles (*40*) suggest that these forests did not have the range of light environments seen in modern multistratal rainforests. By contrast, leaves of the Paleocene Cerrejón flora show the same bimodal distribution of single-taxon VLA and the wide range of cuticle $\delta^{13}C$ observed in modern closed canopy, multistratal forests (*39*, *40*). Maastrichtian wet tropical forests, therefore, likely had an open canopy that promoted mixing of respired and atmospheric CO_2 and a small light gradient between the understory and the canopy compared to modern Neotropical forests. These open canopy forests may have recycled less rainfall through transpiration than their multistratal Paleocene equivalents, potentially influencing regional and global climate (*42*).

Diversity of plant-insect interactions

The diversity of insect-feeding damage on leaves reflects the richness of insect herbivores (*43*). We quantified insect damage in the Guaduas and Bogotá floras following a standard damage type (DT) system and compared it with damage from the Paleocene Cerrejón flora (*18*). Over 50% of leaves in all three floras show insect herbivory (Fig. 4C), indicating intense biotic interactions in both Maastrichtian and Paleocene forests. The richness of insect DTs in the Guaduas flora is comparable to that at Bogotá and greater than at Cerrejón, both for total DT richness resampled at 95% coverage (Guaduas versus Bogotá: 46.5 versus 47.8 DTs, *t* test one-tailed, $t = 0.325$, df = 579, $P = 0.745$; Guaduas versus Cerrejón: 46.5 versus 16.0 DTs, *t* test one-tailed, $t = 6.23$, df = 483, $P < 0.001$) and for specialized damage only (at 90% coverage: Guaduas versus Bogotá: 30.53 versus 29.48 DTs, *t* test, $t = 0.20$, df = 802, $P = 0.841$; Guaduas versus Cerrejón: 30.53 versus 11.43 DTs, *t* test, $t = 5.09$, df = 1121, $P < 0.001$; Fig. 4D).

Because insect-feeding damage reflects inflicting herbivores, DT beta-diversity across host species provides evidence of host specificity among insect herbivore communities. Leaf damage beta-diversity across host taxa in the Maastrichtian Guaduas flora is higher than expected by chance (Wilcoxon test, W = 41615, $P < 0.001$) and higher than that observed at either Bogotá or Cerrejón (Guaduas versus Bogotá: Wilcoxon test, W = 1322, $P < 0.001$; Guaduas versus Cerrejón: Wilcoxon test, W = 1410, $P < 0.001$) (Fig. 4E). This distribution of DTs in the Guaduas flora suggests greater herbivore community specificity than at either Paleocene site.

The end-Cretaceous shaped modern Neotropical rainforests

Prior to the end-Cretaceous, Neotropical rainforests had relatively open canopies; contained a mixture of angiosperms, ferns, and conifers (mostly Araucariaceae); and suffered intense and host-specific insect herbivory. Paleocene forests, by contrast, were more similar to modern Neotropical rainforests in having closed, multistratal canopies, biomass dominated by angiosperms, and a similar plant family composition. Yet, Paleocene rainforests were less diverse than Maastrichtian, Eocene, or modern rainforests (*19*), and the low plant diversity seen throughout the Paleocene shows a long lag in the recovery of diversity following the P/Kg event.

The differences between Maastrichtian and Paleocene forests in floral composition and canopy structure, but similar leaf physiognomy, denote two fundamentally distinct ecosystems that developed under the same wet, tropical climate. Because of their open canopies, lower angiosperm abundance, and a constant, albeit minor, presence of conifers, Maastrichtian rainforests may have been accompanied by slower rates of carbon fixation, transpiration, and nutrient cycling when compared to Paleocene rainforests. In addition, the development of closed canopy rainforests in the Paleocene would have created stronger vertical gradients in light and water use, providing opportunities for new plant habit and growth forms and leading to the vertical complexity seen in modern rainforests.

These notable differences raise two questions: (i) Why did Maastrichtian rainforests lack a closed canopy? By the Late Cretaceous, angiosperms were taxonomically and ecologically diverse (*44*, *45*) and had evolved a wide range of growth habits, ranging from aquatic plants to large trees (*45*, *46*), making it unlikely that they were inherently unable to form a closed canopy. (ii) Why did Paleocene rainforests establish a different plant community composition and structure instead of returning to the Maastrichtian-like rainforests? This is particularly perplexing given the similarity in Paleocene and Maastrichtian climates.

We offer three, non–mutually exclusive explanations for the observed pattern. One is disturbance by large herbivores. Sustained trampling and extensive feeding by large herbivores, mostly dinosaurs (*47*), could have maintained an open canopy by reducing competition for light among neighboring plants through continuous habitat disturbance and gap generation. Such pervasive disturbance could explain the abundance of ferns in Maastrichtian palynofloras, as they typically thrive in successional vegetation (*48*). The extinction of large herbivores at the end-Cretaceous would have reduced gap formation, triggering a "race for light" among tropical plants, and creating more shaded habitats in which a wider variety of light and growth strategies could succeed (*49*). A second explanation involves soil nutrients. Extensive and stable lowlands developed in northern South America during the Maastrichtian (*50*), with a persistent humid climate over millions of years. Maastrichtian forests therefore must have grown on strongly weathered soils characterized by extreme infertility (*51*) with nutrient limitation of growth exacerbated by the high CO_2 concentrations and associated high water-use efficiency that reduces nutrient uptake by mass flow (*52*, *53*). These low-nutrient conditions would have promoted an open canopy structure by favoring the conifers, which in modern tropical forests are typically associated with infertile soils (*54*). Ashfall from the Chicxulub impact added weatherable phosphorus minerals to terrestrial ecosystems worldwide (*55*), instantly resetting fertility to the high-phosphorus, low-nitrogen period that characterizes young stages of ecosystem development (*51*). This set the stage for the diversification of nitrogen-fixing taxa in the Fabaceae, whose rise in the Paleocene (*34*) would have increased soil fertility, stimulated forest productivity (*56*), and enhanced the relative advantage of high–growth-rate angiosperms over conifers and ferns (*57*, *58*). These proposed changes in nutrient cycling could be tested by analyzing paleosol composition and isotopic signatures across the Maastrichtian–Paleocene interval. A third explanation of the observed pattern concerns selective extinction. Although the Araucariaceae were not diverse, they could have been important in structuring the Late Cretaceous canopy environment (*59*). Lineages with narrow ecological ranges and tree growth forms such as Araucariaceae are particularly susceptible to mass extinction events (*60*). By contrast, high ecological diversity within Maastrichtian angiosperm lineages (*44*, *45*) may have made them more resistant to extinction (*60*), as might their higher capacity for whole-genome duplication (*61*–*63*). The near disappearance of conifer trees from tropical rainforest canopies at the end of the Cretaceous may have released resources upon which the modern angiosperm canopy-forming lineages diversified during the Paleocene. This scenario could be tested by assessing shifts in diversification rates across the K/Pg of Neotropical canopy trees, epiphytes, and lianas.

Although there is still much to be learned about the Cretaceous and Paleocene tropical forests, the changes described here show that the end-Cretaceous event had profound consequences for tropical vegetation, ultimately enabling the assembly of modern Neotropical rainforests. It is notable that a single historical

accident altered the ecological and evolutionary trajectory of tropical rainforests, in essence triggering the formation of the most diverse biome on Earth.

REFERENCES AND NOTES

1. T. Westerhold *et al*., *Clim. Past* **13**, 1129–1152 (2017).
2. V. Vajda, A. Bercovici, *Global Planet. Change* **122**, 29–49 (2014).
3. T. R. Lyson *et al*., *Science* **366**, 977–983 (2019).
4. P. M. Hull *et al*., *Science* **367**, 266–272 (2020).
5. K. R. Johnson, *Nature* **366**, 511–512 (1993).
6. V. D. Barreda *et al*., *PLOS ONE* **7**, e52455 (2012).
7. V. Vajda, J. I. Raine, *N. Z. J. Geol. Geophys.* **46**, 255–273 (2003).
8. M. P. Donovan, A. Iglesias, P. Wilf, C. C. Labandeira, N. R. Cúneo, *Nat. Ecol. Evol.* **1**, 12 (2016).
9. A. Iglesias *et al*., *Geology* **35**, 947–950 (2007).
10. D. J. Nichols, in *The Hell Creek Formation and the Cretaceous–Tertiary Boundary in the Northern Great Plains: An Integrated Continental Record of the End of the Cretaceous*. Geological Society of America Special Paper 361, J. H. Hartman, K. R. Johnson, D. J. Nichols, Eds. (2002), pp. 393–456.
11. D. J. Peppe, *Palaeogeogr. Palaeoclimatol. Palaeoecol.* **298**, 224–234 (2010).
12. S. L. Wing, J. Alroy, L. J. Hickey, *Palaeogeogr. Palaeoclimatol. Palaeoecol.* **115**, 117–155 (1995).
13. E. J. M. Koenen *et al*., *Syst. Biol.* 10.1093/sysbio/syaa041 (2020).
14. W. Wang *et al*., *New Phytol.* **195**, 470–478 (2012).
15. S. Ramírez-Barahona, H. Sauquet, S. Magallón, *Nat. Ecol. Evol.* **4**, 1232–1238 (2020).
16. P. R. Renne *et al*., *Geology* **46**, 547–550 (2018).
17. V. Vajda-Santivanez, *Palynology* **23**, 181–196 (1999).
18. See the supplementary materials.
19. S. L. Wing *et al*., *Proc. Natl. Acad. Sci. U.S.A.* **106**, 18627–18632 (2009).
20. J. Alroy, *Proc. Natl. Acad. Sci. U.S.A.* **105** (suppl. 1), 11536–11542 (2008).
21. J. Alroy, The Shifting Balance of Diversity Among Major Marine Animal Groups, *Science* **329**, 1191–1194 (2010).
22. J. Alroy, *Paleobiology* **41**, 633–639 (2015).
23. D. Silvestro, N. Salamin, A. Antonelli, X. Meyer, *Paleobiology* **45**, 546–570 (2019).
24. C. Jaramillo, M. J. Rueda, G. Mora, *Science* **311**, 1893–1896 (2006).
25. C. Jaramillo *et al*., *Science* **330**, 957–961 (2010).
26. A. Rangel, J. M. Moldowan, C. Niño, P. Parra, B. N. Giraldo, *Am. Assoc. Pet. Geol. Bull.* **86**, 2069–2087 (2002).
27. M. A. Caccavari, *Rev. Mus. Argent. Cienc. Nat.* **5**, 135–138 (2003).
28. P. Wilf, S. L. Wing, D. R. Greenwood, C. L. Greenwood, *Geology* **26**, 203–206 (1998).
29. D. J. Peppe *et al*., *New Phytol.* **190**, 724–739 (2011).
30. D. L. Royer *et al*., *Paleobiology* **33**, 574–589 (2007).
31. I. J. Wright *et al*., *Glob. Ecol. Biogeogr.* **14**, 411–421 (2005).
32. E. Correa, C. Jaramillo, S. Manchester, M. Gutierrez, *Am. J. Bot.* **97**, 71–79 (2010).
33. C. Martínez, M. R. Carvalho, S. Madriñán, C. A. Jaramillo, *Am. J. Bot.* **102**, 273–289 (2015).
34. F. Herrera, M. R. Carvalho, S. L. Wing, C. Jaramillo, P. S. Herendeen, *Aust. Syst. Bot.* **32**, 385–408 (2019).
35. M. R. Carvalho, F. A. Herrera, S. Gómez, C. Martínez, C. Jaramillo, *Int. J. Plant Sci.* 10.1086/714053 (2021).
36. R. J. Burnham, *Rev. Palaeobot. Palynol.* **81**, 99–113 (1994).
37. R. Condit *et al*., "Complete data from the Barro Colorado 50-ha plot: 423617 trees, 35 years, 2019 version." (2019); https://datadryad.org/stash/dataset/doi:10.15146/5xcp-0d46.
38. A. Duque *et al*., *Biodivers. Conserv.* **26**, 669–686 (2017).
39. C. Crifó, E. D. Currano, A. Baresch, C. Jaramillo, *Geology* **42**, 919–922 (2014).
40. H. V. Graham, F. Herrera, C. Jaramillo, S. L. Wing, K. H. Freeman, *Geology* **47**, 977–981 (2019).
41. T. S. Feild *et al*., *Proc. Natl. Acad. Sci. U.S.A.* **108**, 8363–8366 (2011).
42. C. K. Boyce, J.-E. Lee, T. S. Feild, T. J. Brodribb, M. Zwieniecki, *Ann. Mo. Bot. Gard.* **97**, 527–540 (2010).
43. M. R. Carvalho *et al*., *PLOS ONE* **9**, e94950 (2014).
44. K. J. Niklas, B. H. Tiffney, A. H. Knoll, in *Phanerozoic Diversity Patterns*, J. W. Valentine, Ed. (Princeton University Press, Princeton, NJ, 1985), pp. 97–128.
45. S. L. Wing, L. D. Boucher, *Annu. Rev. Earth Planet. Sci.* **26**, 379–421 (1998).
46. N. A. Jud *et al*., *Sci. Adv.* **4**, eaar8568 (2018).
47. P. M. Barrett, *Annu. Rev. Earth Planet. Sci.* **42**, 207–230 (2014).
48. S. L. Wing, in *Extinctions in the History of Life*, P. D. Taylor, Ed. (Cambridge Univ. Press, 2004), pp. 61–97.
49. M. Laurans, B. Hérault, G. Vieilledent, G. Vincent, *For. Ecol. Manage.* **329**, 79–88 (2014).
50. L. F. Sarmiento-Rojas, in *Geology and Tectonics of Northwestern South America*, F. Cediel, P. Shaw, Eds. (Springer, 2019), pp. 673–747.
51. T. W. Walker, J. K. Syers, *Geoderma* **15**, 1–19 (1976).
52. L. A. Cernusak, K. Winter, B. L. Turner, *Tree Physiol.* **31**, 878–885 (2011).
53. E. P. McDonald, J. E. Erickson, E. L. Kruger, *Funct. Plant Biol.* **29**, 1115–1120 (2002).
54. T. Jaffré, in *Conifers of the Southern Hemisphere*, N. J. Enright, R. S. Hill, Eds. (Melbourne Univ. Press, 1995), pp. 171–196.
55. D. A. Kring, D. D. Durda, *J. Geophys. Res. Planets* **107**, 5062 (2002).
56. D. Z. Epihov *et al*., *Proc. Biol. Sci.* **284**, 20170370 (2017).
57. D. A. Coomes *et al*., *J. Ecol.* **93**, 918–935 (2005).
58. W. J. Bond, *Biol. J. Linn. Soc. Lond.* **36**, 227–249 (1989).
59. S. V. Wyse, *N. Z. J. Bot.* **50**, 411–421 (2012).
60. W. A. Green, G. Hunt, S. L. Wing, W. A. DiMichele, *Paleobiology* **37**, 72–91 (2011).
61. T. E. Wood *et al*., *Proc. Natl. Acad. Sci. U.S.A.* **106**, 13875–13879 (2009).
62. Z. Li *et al*., *Sci. Adv.* **1**, e1501084 (2015).
63. J. D. Thompson, R. Lumaret, *Trends Ecol. Evol.* **7**, 302–307 (1992).
64. C. Montes *et al*., *Earth Sci. Rev.* **198**, 102903 (2019).
65. C. Jaramillo, Dataset for "The end-Cretaceous and the origin of modern Neotropical rainforests data," figshare (2021); https://doi.org/10.6084/m9.figshare.13611215.v2.

ACKNOWLEDGMENTS

We thank Carbones El Cerrejón, the Montecristo/Peñitas coal mines, and Chechua/Cogua siltstone mines; E. Cadena, A. Rincón, J. Moreno, S. Gómez, D. Carvalho, A. Giraldo, and A. Alfonso for fieldwork assistance; G. Doria and C. Gómez for their work systematizing the fossil collections; three anonymous reviewers for their helpful comments; Universidad del Norte and Museo Mapuka; and Parques Nacionales Naturales de Colombia and Parque Nacional Amacayacu. **Funding:** This research was funded by NSF grant EAR-1829299 (to M.R.C., F.H., C.J.), STRI-Earl S. Tupper postdoctoral fellowship and GSA graduate student research grant (to M.R.C.), the Oak Spring Garden Foundation (to F.H.), Smithsonian Tropical Research Institute, the Anders Foundation, the 1923 Fund and Gregory D. and Jennifer Walston Johnson (to C.J.), the Swiss National Science Foundation and Swedish Research Council (PCEFP3_187012, VR: 2019-04739 to D. Silvestro), and CTFS-ForestGeo. **Author contributions:** C.J. designed and coordinated the research program; M.R.C. and C.J. led the writing with contributions of all coauthors; F.d.l.P., C.D'A., M.R.-B., P.N., M.P.-R., C.J., and C.S. performed palynological data gathering; M.R.C., F.H., S.W., C.M., and M.G. performed paleobotanical analysis; M.R.C. and C.L. performed herbivore analysis; M.R.C., A.D., and D.C. performed analysis of modern vegetation; D.C.R. and C.J. performed pollen data analysis; B.L.T. provided soil expertise; J.L.C. performed radiometric dating; G.B. performed palinspastic reconstruction and sedimentary analysis; and D.S. performed PyRate analysis. **Competing interests:** The authors declare no competing interests. **Data and materials availability:** The data reported and code used in this paper are deposited in figshare digital repository (*65*). Additional information on samples can be accessed using STRI–identification numbers, through https://biogeodb.stri.si.edu/jaramillosdb/web/. The BCI forest dynamics research project was founded by S. P. Hubbell and R. B. Foster and is now managed by R. Perez, S. Aguilar, D. Mitre, and S. Lao under the ForestGEO program of the Smithsonian Tropical Research Institute in Panama. Numerous organizations have provided funding, principally the U.S. National Science Foundation, and hundreds of field workers have contributed.

SUPPLEMENTARY MATERIALS

science.sciencemag.org/content/372/6537/63/suppl/DC1
Materials and Methods
Supplementary text
Figs. S1 to S8
Table S1 to S11
References (*66–114*)
Data S1 to S6

13 October 2020; accepted 3 February 2021
10.1126/science.abf1969

Extinction at the end-Cretaceous and the origin of modern Neotropical rainforests

Mónica R. Carvalho, Carlos Jaramillo, Felipe de la Parra, Dayenari Caballero-Rodríguez, Fabiany Herrera, Scott Wing, Benjamin L. Turner, Carlos D'Apolito, Millerlandy Romero-Báez, Paula Narváez, Camila Martínez, Mauricio Gutierrez, Conrad Labandeira, German Bayona, Milton Rueda, Manuel Paez-Reyes, Dairon Cárdenas, Álvaro Duque, James L. Crowley, Carlos Santos and Daniele Silvestro

Science **372** (6537), 63-68.
DOI: 10.1126/science.abf1969

The birth of modern rainforests

The origin of modern rainforests can be traced to the aftermath of the bolide impact at the end of the Cretaceous. Carvalho *et al.* used fossilized pollen and leaves to characterize the changes that took place in northern South American forests at this time (see the Perspective by Jacobs and Currano). They not only found changes in species composition but were also able to infer changes in forest structure. Extinctions were widespread, especially among gymnosperms. Angiosperm taxa came to dominate the forests over the 6 million years of recovery, when the flora began to resemble that of modern lowland neotropical forest. The leaf data also imply that the forest canopy evolved from relatively open to closed and layered, leading to increased vertical stratification and a greater diversity of plant growth forms.

Science, this issue p. 63; see also p. 28